

# European Journal of Mineralogy

## Lead-antimony sulfosalts from Tuscany (Italy). XXII. Marcobaldiite, $\sim\text{Pb}_{12}(\text{Sb}_3\text{As}_2\text{Bi})\Sigma_6\text{S}_{21}$ , a new member of the jordanite homologous series from the Pollone mine, Valdicastello Carducci --Manuscript Draft--

<b>Manuscript Number:</b>	
<b>Article Type:</b>	Research paper
<b>Full Title:</b>	Lead-antimony sulfosalts from Tuscany (Italy). XXII. Marcobaldiite, $\sim\text{Pb}_{12}(\text{Sb}_3\text{As}_2\text{Bi})\Sigma_6\text{S}_{21}$ , a new member of the jordanite homologous series from the Pollone mine, Valdicastello Carducci
<b>Short Title:</b>	Marcobaldiite, a new jordanite homologue
<b>Corresponding Author:</b>	Cristian Biagioni Universita di Pisa ITALY
<b>Corresponding Author E-Mail:</b>	biagioni@dst.unipi.it
<b>Order of Authors:</b>	Cristian Biagioni Marco Pasero Yves Moelo Federica Zaccarini Werner H. Paar
<b>Abstract:</b>	<p>The new mineral species marcobaldiite, <math>\sim\text{Pb}_{12}(\text{Sb}_3\text{As}_2\text{Bi})\Sigma_6\text{S}_{21}</math>, has been discovered in a single specimen collected in a quartz vein embedded in tourmaline-bearing schists from the Pollone mine, Valdicastello Carducci, Pietrasanta, Apuan Alps, Tuscany, Italy. It occurs as a black blocky prismatic crystal, up to 1 cm in size, with a metallic luster, associated with Sb-rich tennantite. Under the ore microscope, marcobaldiite is white, with a distinct anisotropism, with grey - bluish grey rotation tints. Polysynthetic lamellar twinning is common and characteristic. Reflectance percentages for the four COM wavelengths are [Rmin, Rmax (%), (<math>\lambda</math>): 31.6, 40.1 (470 nm), 30.9, 39.6 (546 nm), 30.4, 38.5 (589 nm), and 30.0, 37.6 (650 nm). Electron microprobe analyses gave (average of 10 spot analyses - in wt%): Pb 64.05(34), As 4.51(8), Sb 9.10(14), Bi 4.24(6), S 17.24(19), total 99.14(53). On the basis of <math>\Sigma\text{Me} = 20</math> apfu, the empirical formula is <math>\text{Pb}_{11.98(4)}\text{Sb}_{2.90(3)}\text{As}_{2.33(3)}\text{Bi}_{0.79(1)}\text{S}_{20.80(20)}</math>. The main diffraction lines, corresponding to multiple hkl indices, are [d in Å (relative visual intensity)]: 3.568 (ms), 3.202 (ms), 3.016 (ms), 2.885 (ms), 2.233 (vs), 2.125 (s), 1.848 (s), and 1.775 (s). The crystal structure study gives a triclinic unit cell, space group P, with <math>a = 8.9248(9)</math>, <math>b = 29.414(3)</math>, <math>c = 8.5301(8)</math> Å, <math>\alpha = 98.336(5)</math>, <math>\beta = 118.175(5)</math>, <math>\gamma = 90.856(5)^\circ</math>, <math>V = 1944.1(3)</math> Å<sup>3</sup>, <math>Z = 2</math>. The crystal structure has been solved and refined to <math>R_1 = 0.067</math> on the basis of 6193 reflections with <math>F_o &gt; 4\sigma(F_o)</math> and 363 refined parameters. Marcobaldiite is a new <math>N = 3.5</math> homologue of the jordanite homologous series, characterized by the 1:1 alternation of two kinds of layers of distorted octahedra, three- and four-octahedra thick, i.e. of the kirkiite and jordanite types, respectively. Layers are connected by one atomic layer of three bicapped trigonal prismatic Pb atoms and one triangular pyramidal As atom in split position. The name of this new mineral species honours the mineral amateur Marco Baldi (b. 1944) for his contribution to the knowledge of the mineralogy of the pyrite <math>\pm</math> baryte <math>\pm</math> iron oxide ore deposits from southern Apuan Alps.</p>
<b>Keywords:</b>	marcobaldiite; new mineral; sulfosalt; crystal structure; lead; antimony; arsenic; bismuth; Pollone mine; Apuan Alps.
<b>Manuscript Region of Origin:</b>	ITALY
<b>Requested Editor:</b>	Sergey V. Krivovichev, Editor-in-Chief
<b>Suggested Reviewers:</b>	Emil Makovicky University of Copenhagen

	emilm@ign.ku.dk
	Tonci Balic Zunic University of Copenhagen toncib@ign.ku.dk
	Yoshitaka Matsushita National Institute for Materials Science Matsushita.Yoshitaka@nims.go.jp
<b>Opposed Reviewers:</b>	
<b>Additional Information:</b>	
<b>Question</b>	<b>Response</b>
<b>Author Comments:</b>	



July 4, 2017

Manuscript

Dear Sir,

we would like to publish our paper in *European Journal of Mineralogy*.

The paper, entitled “**Lead-antimony sulfosalts from Tuscany (Italy). XXII. Marcobaldiite,  $\sim\text{Pb}_{12}(\text{Sb}_3\text{As}_2\text{Bi})_{\Sigma 6}\text{S}_{21}$ , a new member of the jordanite homologous series from the Pollone mine, Valdicastello Carducci**” has not been previously published and it will not be submitted elsewhere for publication while it is in review for *European Journal of Mineralogy*.

Marcobaldiite is a new  $N = 3.5$  homologue in the jordanite homologous series and shows a new kind of crystal structure. The approval of marcobaldiite as a valid mineral species has been voted by the IMA CNMNC (IMA 2015-109).

Yours faithfully,

Cristian Biagioni

1 **Title:** Lead-antimony sulfosalts from Tuscany (Italy). XXII. Marcobaldiite,  $\sim\text{Pb}_{12}(\text{Sb}_3\text{As}_2\text{Bi})_{\Sigma 6}\text{S}_{21}$ , a  
2 new member of the jordanite homologous series from the Pollone mine, Valdicastello  
3 Carducci

4

5 **Running title:** Marcobaldiite, a new jordanite homologue

6

7 **Plan of the article:**

8 Abstract

9 1. Introduction

10 2. Geological setting

11 3. Occurrence and mineral description

12 3.1. Chemical data

13 3.2. Crystallography

14 4. Crystal structure description

15 4.1. General organization

16 4.2. Cation coordinations and site occupancies

17 5. Discussion

18 5.1. Structural formula

19 5.2. Bismuth in the jordanite homologous series

20 5.3. Conditions of formation

21 6. Conclusion

22 References

23

24 **Corresponding author:** Cristian Biagioni

25 **Computer:** PC

26 **OS:** Windows

27 **Software:** Word

28 **Number of characters** (including spaces): 36852

29

30 **Lead-antimony sulfosalts from Tuscany (Italy). XXII.**  
31 **Marcobaldiite, ~ Pb<sub>12</sub>(Sb<sub>3</sub>As<sub>2</sub>Bi)<sub>Σ6</sub>S<sub>21</sub>, a new member of**  
32 **the jordanite homologous series from the Pollone mine,**  
33 **Valdicastello Carducci**

34  
35 CRISTIAN BIAGIONI<sup>1,\*</sup> MARCO PASERO<sup>1</sup>, YVES MOËLO<sup>2</sup>, FEDERICA ZACCARINI<sup>3</sup>, and  
36 WERNER H. PAAR<sup>4</sup>

37  
38 <sup>1</sup>Dipartimento di Scienze della Terra, Università di Pisa, Via S. Maria 53, I-56126 Pisa, Italy

39 <sup>2</sup>Institut des Matériaux Jean Rouxel (IMN), Université de Nantes, CNRS, 2, rue de la Houssinière,  
40 BP 32229, F-44322 Nantes Cedex 3, France

41 <sup>3</sup>Resource Mineralogy, University of Leoben, Peter Tunner Str. 5, A-8700 Leoben, Austria

42 <sup>4</sup>Department of Chemistry and Physics of Materials, University, Hellbrunnerstr. 34, A-5020  
43 Salzburg, Austria

44  
45 \*Corresponding author, e-mail: [cristian.biagioni@unipi.it](mailto:cristian.biagioni@unipi.it)

47 **Abstract:** The new mineral species marcobaldiite,  $\sim \text{Pb}_{12}(\text{Sb}_3\text{As}_2\text{Bi})_{\Sigma 6}\text{S}_{21}$ , has been discovered in a  
48 single specimen collected in a quartz vein embedded in tourmaline-bearing schists from the Pollone  
49 mine, Valdicastello Carducci, Pietrasanta, Apuan Alps, Tuscany, Italy. It occurs as a black blocky  
50 prismatic crystal, up to 1 cm in size, with a metallic luster, associated with Sb-rich tennantite. Under  
51 the ore microscope, marcobaldiite is white, with a distinct anisotropism, with grey – bluish grey  
52 rotation tints. Polysynthetic lamellar twinning is common and characteristic. Reflectance  
53 percentages for the four COM wavelengths are [ $R_{\min}$ ,  $R_{\max}$  (%), ( $\lambda$ ): 31.6, 40.1 (470 nm), 30.9, 39.6  
54 (546 nm), 30.4, 38.5 (589 nm), and 30.0, 37.6 (650 nm). Electron microprobe analyses gave  
55 (average of 10 spot analyses – in wt%): Pb 64.05(34), As 4.51(8), Sb 9.10(14), Bi 4.24(6), S  
56 17.24(19), total 99.14(53). On the basis of  $\Sigma Me = 20$  apfu, the empirical formula is  
57  $\text{Pb}_{11.98(4)}\text{Sb}_{2.90(3)}\text{As}_{2.33(3)}\text{Bi}_{0.79(1)}\text{S}_{20.80(20)}$ . The main diffraction lines, corresponding to multiple  $hkl$   
58 indices, are [ $d$  in Å (relative visual intensity)]: 3.568 (ms), 3.202 (ms), 3.016 (ms), 2.885 (ms),  
59 2.233 (vs), 2.125 (s), 1.848 (s), and 1.775 (s). The crystal structure study gives a triclinic unit cell,  
60 space group  $P\bar{1}$ , with  $a = 8.9248(9)$ ,  $b = 29.414(3)$ ,  $c = 8.5301(8)$  Å,  $\alpha = 98.336(5)$ ,  $\beta = 118.175(5)$ ,  
61  $\gamma = 90.856(5)^\circ$ ,  $V = 1944.1(3)$  Å<sup>3</sup>,  $Z = 2$ . The crystal structure has been solved and refined to  $R_1 =$   
62 0.067 on the basis of 6193 reflections with  $F_o > 4\sigma(F_o)$  and 363 refined parameters. Marcobaldiite is  
63 a new  $N = 3.5$  homologue of the jordanite homologous series, characterized by the 1:1 alternation of  
64 two kinds of layers of distorted octahedra, three- and four-octahedra thick, *i.e.* of the kirkiite and  
65 jordanite types, respectively. Layers are connected by one atomic layer of three bicapped trigonal  
66 prismatic Pb atoms and one triangular pyramidal As atom in split position. The name of this new  
67 mineral species honours the mineral amateur Marco Baldi (b. 1944) for his contribution to the  
68 knowledge of the mineralogy of the pyrite  $\pm$  baryte  $\pm$  iron oxide ore deposits from southern Apuan  
69 Alps.

70 **Key-words:** marcobaldiite; new mineral; sulfosalt; crystal structure; lead; antimony; arsenic;  
71 bismuth; Pollone mine; Apuan Alps.

72

## 73 1. Introduction

74 The jordanite homologous series, first defined by Makovicky (1989), is a group of lead  
75 sulfosalts having general formula  $\text{Pb}_{4N-2}\text{Me}^{3+}_6\text{S}_{4N+7}$ , where  $\text{Me}^{3+} = \text{As}, \text{Sb}, \text{Bi}$  (Makovicky *et al.*,  
76 2006). Three mineral species belonging to this series are reported in Moëlo *et al.* (2008), *i.e.*  
77 jordanite, geocronite, and kirkiite. The possibly related mineral tsugaruite, ideally  $\text{Pb}_4\text{As}_2\text{S}_7$   
78 (Shimizu *et al.*, 1998), has a different crystal structure (Matsushita *et al.*, 2014), even if its details  
79 have not been published yet.

80 Jordanite homologues are characterized by two short axes ( $\sim 8.5$  and  $\sim 9.0$  Å) and a longer one,  
81 whose length depends on the homologue order, ranging from  $\approx 26$  Å ( $N = 3$  – kirkiite) to  $\approx 32$  Å ( $N$   
82  $= 4$  – jordanite and geocronite). The  $N = 4$  isotypic pair jordanite ( $\text{Pb}_{14}\text{As}_6\text{S}_{23}$ ) – geocronite  
83 ( $\text{Pb}_{14}\text{Sb}_6\text{S}_{23}$ ) is well-known from various localities world-wide, and, considering also synthetic  
84 products (Jambor, 1969), displays a complete solid-solution. On the contrary, kirkiite, ideally  
85  $\text{Pb}_{10}\text{As}_3\text{Bi}_3\text{S}_{19}$ , is exceedingly rare, having been described only in two localities, the Greek type  
86 locality (the Pb-Zn ore deposit of Aghios Philippos, near Kirki, Thrace; Moëlo *et al.*, 1985), and the  
87 high- $T$  fumaroles of La Fossa crater, Vulcano, Aeolian Islands, Italy (Borodaev *et al.*, 1998; Pinto *et*  
88 *al.*, 2006).

89 In order to fully characterize the occurrence of geocronite from the Pollone mine, near the  
90 small hamlet of Valdicastello Carducci, Apuan Alps, Italy, where this mineral has been known  
91 since the first description given by Kerndt (1845), Biagioni *et al.* (2016a) examined both historical  
92 and new samples from this locality, studying them through single-crystal X-ray diffraction and  
93 electron-microprobe analysis. During this investigation, a mineral was found having the two short  
94 unit-cell parameters close to those of jordanite homologues and the longer one intermediate  
95 between those of the  $N = 3$  and  $N = 4$  members, *i.e.*  $\approx 29$  Å. The crystallographic and chemical  
96 studies allowed its identification as a new homologue belonging to the jordanite series, *i.e.*  
97 marcobaldiite, with  $N = 3.5$  homologue number. The new mineral and its name have been approved  
98 by the CNMNC-IMA (2015-109). The holotype material is deposited in the mineralogical  
99 collections of the Museo di Storia Naturale, Università di Pisa, Via Roma 79, Calci, Pisa, Italy,  
100 under catalogue number 19709. The name is in honour of the mineral collector Marco Baldi (b.  
101 1944), for his contribution to the knowledge of the mineralogy of the pyrite  $\pm$  baryte  $\pm$  iron oxide  
102 ore deposits from southern Apuan Alps. Marco Baldi was the first to describe the actual occurrence  
103 of geocronite crystals from Valdicastello Carducci (Baldi, 1982). His contribution favored the  
104 mineralogical rediscovery of the Pollone mine, which since then has been explored by mineral  
105 collectors and mineralogists, leading to the discovery of several rare and new mineral species,

106 mainly represented by lead sulfosalts (sterryite, parasterryite, carducciite, meerschautite, and  
107 polloneite – Moëlo *et al.*, 2011; Biagioni *et al.*, 2014; Biagioni *et al.*, 2016b; Topa *et al.*, 2017).

108 The aim of this paper is the full description of the new mineral species marcobaldiite and the  
109 discussion of its crystal-chemistry in the framework of the jordanite homologous series.

110

## 111 **2. Geological setting**

112 The baryte + pyrite ± (Pb-Zn-Ag) Pollone ore deposit (latitude 43°57'47''N, longitude  
113 10°16'19''E) is located near the small hamlet of Valdicastello Carducci, Pietrasanta, Tuscany, Italy.  
114 The ore bodies are hosted within a Paleozoic metavolcanic-metasedimentary sequence,  
115 metamorphosed up to greenschist facies conditions during the Alpine orogeny. Estimates of *P-T*  
116 conditions indicate metamorphic temperatures up to 350°C with a pressure of 0.35 GPa. Higher *T*  
117 values (450°C) were recorded for mineralizing fluids (Costagliola *et al.*, 1998). Biagioni *et al.*  
118 (2016a) described the main geological and structural features of the Pollone mine and distinguished  
119 three kinds of occurrence: *i*) lenses of microcrystalline baryte + pyrite, with the local presence of  
120 interlayers/lenses of galena + sphalerite, folded and partially re-worked during the late tectonic  
121 stage evolution of Apuan Alps metamorphic complex (*e.g.*, Carmignani & Kligfield, 1990); *ii*)  
122 quartz lensoid veins, oriented SW-NE, with coarse-grained masses of galena, sphalerite, and  
123 sulfosalts; and *iii*) extension quartz ± baryte ± sulfides veins, trending N140-170, embedded both in  
124 the country rocks and in the ore bodies.

125 Twenty-four different sulfosalts have been identified in the Pollone ore deposit (Table 1). The  
126 typical occurrence is represented by the microcrystalline baryte + pyrite ore bodies, where sulfosalts  
127 are scattered as interstitial grains or as euhedral prismatic to acicular individuals. Rarely, they are  
128 related to small quartz + baryte veinlets and small fissures occurring in these ore bodies. This kind  
129 of occurrence is typical for the lead-silver sulfosalts typical of the Pollone mine. The quartz ±  
130 baryte ± sulfides extension veins represent another source of sulfosalts. Actually, the well-  
131 crystallized specimens of jordanite and geocronite were found in the vugs of these veins. Finally,  
132 some Ag sulfosalts have been identified in the quartz lensoid veins oriented SW-NE (*i.e.*, diaphorite  
133 and pyrargyrite – Frizzo & Simone, 1995).

134 Marcobaldiite was found in a quartz extension vein embedded in tourmaline-rich schist,  
135 occurring in the Stanzone tunnel, one of the stopes of the Pollone mine. Its crystallization is related  
136 to the circulation of hydrothermal fluids during the Tertiary Alpine tectono-metamorphic events,  
137 favoring the remobilization of elements from the country rocks and the ore bodies and their  
138 crystallization in the extension veins (Biagioni *et al.*, 2016a).

139



### 140 3. Occurrence and mineral description

141 Marcobaldiite was identified in only one sample collected in quartz extension veins; in the  
142 same vein Sb-rich tennantite was identified. It occurs as a black prismatic crystal measuring 10×3×3  
143 mm. The presence of striations suggests the occurrence of a polysynthetic twinning, confirmed by  
144 reflected light microscopy (see below). It is brittle, with an irregular fracture. The streak is black,  
145 the luster is metallic.

146 Micro-indentation measurements carried out with a VHN load of 15 g give a mean value of  
147 182 kg mm<sup>-2</sup> (range: 170 – 195 kg mm<sup>-2</sup>), corresponding to a Mohs hardness of ~ 3–3½. Density  
148 was not measured; calculated density is 6.56 g cm<sup>-3</sup>, on the basis of the empirical formula.

149 In plane-polarized incident light, marcobaldiite is white in color, distinctly bireflectant.  
150 Between crossed polars, it is anisotropic, with grey to bluish-grey rotation tints. Internal reflections  
151 were not observed. Polysynthetic twinning is common and characteristic (Fig. 1). The reflectance  
152 values of marcobaldiite were determined in air with WTiC as standard (Table 2).

153

#### 154 3.1. Chemical analysis

155 A grain of marcobaldiite was analyzed with a Superprobe JEOL JXA 8200 electron  
156 microprobe (Eugen F. Stumpfl laboratory, Leoben University, Austria). The operating conditions  
157 (WDS mode) were: accelerating voltage 20 kV, beam current 10 nA, beam size 1 µm. Standards  
158 (element, emission line) were: galena (Pb *Mα*), stibnite (Sb *Lα*), GaAs (As *Lα*), pyrite (S *Kα*), and  
159 Bi<sub>2</sub>Te<sub>3</sub> (Bi *Mα*). Counting times were 30 s on the peak and 15 s on the right and left backgrounds.  
160 The studied grain proved to be very homogeneous. Chemical data are given in Table 3.

161 On the basis of  $\Sigma Me = 18$  atoms per formula unit (*apfu*), the empirical formula of  
162 marcobaldiite is Pb<sub>11.98</sub>Sb<sub>2.90</sub>As<sub>2.33</sub>Bi<sub>0.79</sub>S<sub>20.80</sub>. The idealized stoichiometric chemical formula of the  
163 studied sample is Pb<sub>12</sub>(Sb<sub>3</sub>As<sub>2</sub>Bi)<sub>Σ6</sub>S<sub>21</sub>, corresponding to (in wt%) Pb 64.02, Sb 9.40, As 3.86, Bi  
164 5.38, S17.34, sum 100.00.

165

#### 166 3.2. Crystallography

167 X-ray powder diffraction (XRPD) pattern of marcobaldiite was collected using a 114.6 mm  
168 Gandolfi camera with Ni-filtered Cu *Kα* radiation. The observed pattern, compared with the  
169 calculated one (obtained using the software PowderCell; Kraus & Nolze, 1996) is reported in Table  
170 4. Owing to the multiplicity of indices for the majority of the observed diffraction lines, the unit-cell  
171 parameters were not refined from X-ray powder diffraction data.

172 Single-crystal X-ray intensity data collection was performed using a Bruker Smart Breeze  
173 diffractometer (50 kV, 30 mA) equipped with a CCD 4k low noise area detector. Graphite

174 monochromatized Mo  $K\alpha$  radiation was used. The detector-to-crystal working distance was 50 mm.  
175 6008 frames were collected in  $\omega$  scan modes, in  $0.25^\circ$  slices. Exposure time was 25 s per frame. The  
176 data were integrated and corrected for Lorentz-polarization, background effects, and absorption,  
177 using the package of software *Apex2* (Bruker AXS Inc., 2004), resulting in a set of 6794  
178 independent reflections. The refined unit-cell parameters are  $a = 8.9248(9)$ ,  $b = 29.414(3)$ ,  $c =$   
179  $8.5301(8)$  Å,  $\alpha = 98.336(5)$ ,  $\beta = 118.175(5)$ ,  $\gamma = 90.856(5)^\circ$ ,  $V = 1944.1(3)$  Å<sup>3</sup>. The statistical tests  
180 on  $|E|$  values ( $|E^2 - 1| = 0.993$ ) suggested the possible centrosymmetry of marcobaldiite.  
181 Consequently, the crystal structure was solved in the space group  $P\bar{1}$  using *Shelxs-97* (Sheldrick,  
182 2008). Scattering curves for neutral atoms were taken from the *International Tables for*  
183 *Crystallography* (Wilson, 1992).

184 In a first step, the positions of the heavier atoms (Pb, Bi, Sb) were found; through successive  
185 difference-Fourier maps, the other atom positions were located. In the crystal structure of  
186 marcobaldiite, there are eighteen independent cation positions (one of them split) and twenty-one S  
187 sites. Among cation sites, twelve Pb positions and six (Sb/As) sites were identified on the basis of  
188 site scattering and  $Me-S$  distances. The site occupancy factors (s.o.f.) of the Pb positions were  
189 initially refined using the scattering curve of Pb vs  $\square$  and they were found to be fully occupied. The  
190 six (Sb/As) positions were refined using the scattering curves of Sb vs As. Whereas four of them are  
191 mixed (Sb/As) positions, with variable As and Sb contents, Sb4 was found to be completely  
192 occupied by Sb only, whereas an atom heavier than Sb partially occupies the Pb9 site.  
193 Consequently, the s.o.f. of this site was modeled using the curve of Pb and Sb, giving a s.o.f.  
194  $Pb_{0.61}Sb_{0.39}$ . After several cycles of isotropic refinement using *Shelxl-2014* (Sheldrick, 2015), the  $R_1$   
195 converged to 0.087. By refining the anisotropic displacement parameters for cations only, the  
196 refinement yielded a  $R_1$  value of 0.071.

197 Chemical analysis showed the presence of 0.79 Bi *apfu*. Owing to the similar scattering  
198 factors of Pb ( $Z = 82$ ) and Bi ( $Z = 83$ ), it is not possible to distinguish these two atoms on the basis  
199 of the site scattering. On the contrary, their bond valence sums (BVS), calculated using the bond  
200 parameters of Brese & O'Keeffe (1991), were taken into account. An examination of the BVS at the  
201 different Pb and (Pb/Sb) sites suggests that Bi is not preferentially partitioned at any specific  
202 position, but it would be statistically distributed among some Pb positions. Bismuth was located  
203 in the four Pb sites having the highest BVS values, *i.e.* Pb1, Pb8, Pb15, and Pb16, with a Bi content  
204 not over-passing 0.15 *apfu* in each position. The BVS at the Pb9 position agrees with a mixed  
205 (Pb,Sb) occupancy, and not with a mixed (Bi,Sb) or (Pb,Sb,Bi) occupancy.

206 The final anisotropic model for all the atom positions gave  $R_1 = 0.067$  for 6193 reflections  
207 with  $F_o > 4\sigma(F_o)$  and 363 refined parameters. Further details of data collection and refinement are

208 given in Table 5. Atomic coordinates and equivalent isotropic displacement parameters of  
209 marcobaldiite are given in Table 6. The unit cell is represented in Fig. 2.

210

## 211 **4. Crystal structure description**

### 212 **4.1. General organization**

213 Marcobaldiite is the  $N = 3.5$  member of the jordanite homologous series. Following the  
214 modular description given by Makovicky *et al.* (2006) for the  $N = 3$  homologue kirkiite, the crystal  
215 structure of marcobaldiite (Fig. 3) can be described as formed by a stacking sequence of distorted  
216 layers of octahedra and trigonal prismatic layers parallel to {010} and sharing S atoms along their  
217 boundaries.  $N = 3$  kirkiite-type layers and  $N = 4$  jordanite-type layers, three- and four-octahedra  
218 thick respectively, alternate along [010] in a 1:1 ratio, separated by one atomic slab of three  
219 bicapped trigonal prismatic (Pb,Bi) atoms and one triangular pyramidal As atom (split position).

220 Alternatively, the crystal structure can be described as formed by (111) slabs of distorted PbS  
221 archetype (*e.g.*, Moëlo *et al.*, 1985; Makovicky, 1989), or (210) slabs of SnS archetype. The  
222 broadness of the two kinds of octahedral layer corresponds to three and four subcells of SnS or PbS.  
223 Within each layer, lone-electron-pairs of trivalent Sb and As, at the opposite side of shortest (*i.e.*  
224 strongest) (Sb,As)–S bonds, are directed towards a common oblique interspace, to form so-called  
225 lone-electron-pair micelles (Fig. 3).

226

### 227 **4.2. Cation coordinations and site occupancies**

228 Among cation positions, there are twelve Pb or mixed (Pb,Bi) sites, one pure Sb position, a  
229 mixed (Pb,Sb) site, one pure split As position, and three mixed (Sb/As) sites with different  
230 As/(As+Sb) atomic ratios. Cation characteristics (coordination, mean bond distance, and bond  
231 valence sum) are summarized in Table 7, while bond valence sums on S atoms are given in Table 8.

232 Lead atoms are six- to eight-fold coordinated, with average bond distances ranging from  
233 2.996 Å for the six-fold coordinated Pb10 site to 3.075 Å for the eight-fold coordinated Pb16  
234 position. Pb3, Pb6, Pb10, and Pb11 have a distorted octahedral coordination; actually, the  
235 coordination number of the latter site is increased to seven when S21b site is occupied. These Pb  
236 sites have a pure Pb occupancy, in agreement with their BVS ranging from 1.95 to 1.99 valence unit  
237 (*v.u.*). Pb18 have a six-fold coordination corresponding to a trigonal prismatic polyhedron; two  
238 additional very long Pb–S bonds, ranging between 3.83 and 3.91 Å, give rise to a bicapped trigonal  
239 prism. The Pb atom hosted at this position is underbonded, with a BVS of 1.75 *v.u.* A seven-fold  
240 coordination is shown by Pb1, Pb2, Pb7, Pb8, and Pb14 (when S21a is occupied). The occupancies  
241 of these sites are represented by Pb only (Pb2, Pb7, and Pb14 sites) or by Pb and Bi atoms (Pb1 and

242 Pb8), with a 85:15 atomic ratio. These agree with the BVS calculation, resulting in values ranging  
243 from 1.95 to 2.02 *v.u.* for the pure Pb sites and BVS of 2.10 and 2.08 *v.u.* for the mixed (Pb,Bi).  
244 Finally, the Pb15 and Pb16 sites have a bicapped trigonal prismatic coordination and a mixed  
245 (Pb<sub>0.85</sub>Bi<sub>0.15</sub>) site occupancy. Their BVS values are both 2.10 *v.u.*

246 Five *Me*<sup>3+</sup> positions occur in the crystal structure of marcobaldiite, *i.e.* Sb4, Sb12, As5, As13,  
247 and the split site As17. Taking into account the shortest *Me*–S distances (= the strongest bonds: *Me*–  
248 S < 2.70 Å), these sites display a trigonal pyramidal coordination, with *Me* occupying the apex of  
249 the pyramid. The coordination sphere is completed by three additional longer bonds. Sb4 is a pure  
250 Sb position, with an average <*Me*–S> distance of 2.504 Å and a BVS of 2.94 *v.u.*. Antimony is  
251 dominant also at the Sb12 position, having a refined site occupancy factor (s.o.f.) of Sb<sub>0.98</sub>As<sub>0.02</sub>.  
252 The average <*Me*–S> distance is 2.462 Å and the BVS indicates moderate overbonding (3.14 *v.u.*).  
253 As5, As13, and As17 are three As-dominant positions showing increasing As contents. Indeed, the  
254 refined s.o.f. point to As<sub>0.63</sub>Sb<sub>0.37</sub>, As<sub>0.91</sub>Sb<sub>0.09</sub>, and As<sub>1.00</sub>, respectively. Actually, the As17 site is  
255 split into two sub-positions (As17a and As17b) having a partial occupancy (0.75 and 0.25,  
256 respectively) in order to avoid too-short *Me*–*Me* distances. S21 is also split in two sub-positions  
257 S21a and S21b, with s.o.f. 0.75 and 0.25, respectively. As a consequence, As17a, shift towards the  
258 *N* = 3 layer, is bound to S21a, and As17b to S21b.

259 The refined s.o.f. at As5 and As13 result in relatively high BVS (3.15 and 3.11 *v.u.*,  
260 respectively). The higher As contents are coupled with decreasing mean <*Me*–S> distances (2.325  
261 and 2.262 Å for As5 and As13, respectively). The mean bond distances observed at the As17 sub-  
262 sites are shorter than the ideal one, owing the average nature of the ligand positions, related to the  
263 statistical occupancy of such positions. This explains the too high BVS obtained (3.22 and 3.52  
264 *v.u.*).

265 The crystal structure of marcobaldiite is completed by the mixed (Pb,Sb)9 position, within the  
266 *N* = 4 layer, having a distorted octahedral coordination and an average bond distance of 2.922 Å.  
267 The refined s.o.f. points to a site occupancy Pb<sub>0.61</sub>Sb<sub>0.39</sub>. The calculated BVS, 2.35 *v.u.*, fits the  
268 theoretical one, *i.e.* 2.39 *v.u.*

269

## 270 **5. Crystal-chemistry of jordanite homologues**

### 271 **5.1. Structural formula**

272 As described above, the crystal structure of marcobaldiite (Fig. 3) can be considered as a 1:1  
273 alternation of *N* = 3 (kirkiite-type) and *N* = 4 (jordanite-type) octahedral layers, separated by a layer  
274 formed by Pb trigonal prismatic polyhedra and one As trigonal pyramid (Fig. 2). The *N* = 3 layer of  
275 marcobaldiite has chemical composition [Pb<sub>3</sub>(Pb<sub>0.85</sub>Bi<sub>0.15</sub>)(Sb<sub>1.37</sub>As<sub>0.63</sub>)<sub>Σ2</sub>S<sub>8</sub>]<sup>-1.85</sup>. This chemistry can

276 be compared with that given by Makovicky *et al.* (2006) for the  $N = 3$  octahedral layer in kirkiite,  
 277 *i.e.*  $[\text{Pb}_3(\text{Pb}_{0.75}\text{Bi}_{0.25})(\text{As}_{1.42}\text{Bi}_{0.58})_{\Sigma 2}\text{S}_8]^{-1.75}$ . Figure 4 (top) shows the comparison between the  $N = 3$   
 278 layers in marcobaldiite and kirkiite, whereas the site occupancies are compared in Table 9. The  $N =$   
 279 4 layer (Fig. 4, bottom) has chemical composition  $[\text{Pb}_4(\text{Pb}_{0.85}\text{Bi}_{0.15})(\text{Pb}_{0.61}\text{Sb}_{0.39})(\text{Sb}_{1.07}\text{As}_{0.93})_{\Sigma 2}\text{S}_{10}]^{-1.46}$   
 280 and can be compared with that of jordanite isotypes from the Pollone mine (Biagioni *et al.*, 2016a),  
 281 having a chemistry  $[\text{Pb}_5(\text{Pb}_{0.50}\text{Sb}_{0.50})(\text{Sb}_{0.61-1.23}\text{As}_{1.39-0.77})_{\Sigma 2}\text{S}_{10}]^{-1.5}$ . Finally, the layer composed by Pb  
 282 trigonal prisms and split As site has chemical composition  $[\text{Pb}(\text{Pb}_{0.85}\text{Bi}_{0.15})_2\text{AsS}_3]^{+3.3}$ , to be  
 283 compared with  $[\text{Pb}_3\text{AsS}_3]^{+3}$  in jordanite homologues and  $[\text{Pb}_2(\text{Pb}_{0.50}\text{Bi}_{0.50})\text{AsS}_3]^{+3.5}$  in kirkiite.

284 The crystal-chemical formula of marcobaldiite can be obtained by the sum of the chemical  
 285 compositions of the  $N = 3$ ,  $N = 4$  and the trigonal prismatic atomic layer:  
 286  $[\text{Pb}_3(\text{Pb}_{0.85}\text{Bi}_{0.15})(\text{Sb}_{1.37}\text{As}_{0.63})_{\Sigma 2}\text{S}_8]^{-1.85} + [\text{Pb}_4(\text{Pb}_{0.85}\text{Bi}_{0.15})(\text{Pb}_{0.61}\text{Sb}_{0.39})(\text{Sb}_{1.07}\text{As}_{0.93})_{\Sigma 2}\text{S}_{10}]^{-1.46} +$   
 287  $[\text{Pb}(\text{Pb}_{0.85}\text{Bi}_{0.15})_2\text{AsS}_3]^{+3.30} = \text{Pb}_8(\text{Pb}_{0.85}\text{Bi}_{0.15})_4(\text{Pb}_{0.61}\text{Sb}_{0.39})(\text{As}_{2.56}\text{Sb}_{2.44})_{\Sigma 5.00}\text{S}_{21}$ , that is  
 288  $\text{Pb}_{12.01}(\text{Sb}_{2.83}\text{As}_{2.44}\text{Bi}_{0.60})_{\Sigma 5.99}\text{S}_{21}$ , to be compared with the formula obtained through chemical  
 289 analysis, *i.e.*  $\text{Pb}_{11.98}(\text{Sb}_{2.90}\text{As}_{2.33}\text{Bi}_{0.79})_{\Sigma 6.02}\text{S}_{20.80(20)}$ . It is close to the ideal stoichiometric formula  
 290  $\text{Pb}_{12}(\text{Sb}_3\text{As}_2\text{Bi})\text{S}_{21}$ .

291 All known compositions of jordanite homologues have been represented in the As-Sb-Bi  
 292 sub-system (Fig. 5). Taking into account the ideal formulae of geocronite,  $\text{Pb}_{14}\text{Sb}_6\text{S}_{23}$ , and As-rich  
 293 kirkiite,  $\text{Pb}_{10}\text{As}_4\text{Bi}_2\text{S}_{19}$ , one can see that the ideal formula of marcobaldiite is quite identical to the  
 294 1:1 mixture of these homologues, having formula  $\text{Pb}_{24}(\text{Sb}_6\text{As}_4\text{Bi}_2)\text{S}_{42} = 2 \times \text{Pb}_{12}(\text{Sb}_3\text{As}_2\text{Bi})\text{S}_{21}$ .

295 Since Bi is not dominant at any site of the crystal structure of marcobaldiite, the structural  
 296 formula derived through the single-crystal study could be reduced to a stoichiometric one taking  
 297 into account the coupled substitution  $\text{Pb}^{2+} + \text{Sb}^{3+} = \text{Bi}^{3+} + \text{Pb}^{2+}$ . Indeed, *ca.* 0.60 Bi *apfu* are  
 298 distributed among four Pb positions (*i.e.*, Pb1, Pb8, Pb15, and Pb16), whereas Sb is replaced by *ca.*  
 299 0.60 Pb *apfu* at the Pb9 position. Subtracting Bi, the structural formula become  
 300  $\text{Pb}_{12}(\text{Sb}_{3.44}\text{As}_{2.56})_{\Sigma 6}\text{S}_{21}$ .

301

## 302 5.2. Bismuth in the jordanite homologous series

303 The occurrence of relatively high contents of Bi in this new mineral species is a rare feature  
 304 shown by jordanite homologues. Indeed, the findings of high Bi contents in these minerals are  
 305 limited to three localities, *i.e.* Aghios Philippos, Kirki, Thrace, Greece (Moëlo *et al.*, 1985; Moëlo *et*  
 306 *al.*, 1990); La Fossa crater, Vulcano, Aeolian Islands, Italy (Borodaev *et al.*, 1998; Pinto *et al.*,  
 307 2006); and the Pollone mine, Apuan Alps, Tuscany, Italy.

308 Kirkiite shows Bi contents up to 15.5 and 18.27 wt% in samples from Kirki and Vulcano,  
 309 respectively (Moëlo *et al.*, 1985; Pinto *et al.*, 2006), corresponding to a maximum content of 3.09

310 Bi *apfu*, close to the ideal formula  $\text{Pb}_{10}\text{As}_3\text{Bi}_3\text{S}_{19}$  (Fig. 5). Moreover, Moëlo *et al.* (1990) reported  
311 the identification of an Sb-bearing variety of kirkiite, with two samples having average chemical  
312 compositions of  $\text{Pb}_{10.21}(\text{As}_{3.48}\text{Sb}_{1.36}\text{Bi}_{1.16})\text{S}_{19.70}$  and  $\text{Pb}_{10.27}(\text{As}_{3.89}\text{Sb}_{1.05}\text{Bi}_{1.05})\text{S}_{19.90}$  (Fig. 5), ideally  
313 close to  $\text{Pb}_{10}(\text{As}_4\text{SbBi})\text{S}_{19}$ . This is the lowest Bi content reported for the  $N = 3$  homologue of the  
314 jordanite series. The solution of the crystal structure of kirkiite by Makovicky *et al.* (2006) could  
315 suggest the cross-substitution of Pb and Bi at the Pb4 and Pb6 positions, with Bi being  
316 preferentially partitioned at the Bi1/As1 split site. The chemical variability reported by Moëlo *et al.*  
317 (1985, 1990) could be interpreted in the light of this crystal-chemical behaviour, with the  
318 composition of the Sb-rich variety corresponding to the occurrence of a mixed ( $\text{Bi}_{0.50}\text{Sb}_{0.50}$ )  
319 occupancy at the Bi1/As1 site of Makovicky *et al.* (2006). In conclusion, available chemical data  
320 suggests that Bi is always present in the  $N = 3$  homologue kirkiite.

321 On the contrary, the  $N = 4$  homologues are usually Bi-poor, with Bi contents less up *ca.* 0.50  
322 wt% (*e.g.*, Pollone mine, Apuan Alps, Italy – Biagioni *et al.*, 2016a; Darasun ore deposit, Eastern  
323 Transbaikalia, Russia – Bryzgalov *et al.*, 2011). The highest Bi contents were reported by Moëlo *et al.*  
324 (1985) on a sample of jordanite associated with type kirkiite, containing up to 4.6 wt% Bi,  
325 corresponding to an ideal formula  $\text{Pb}_{14}\text{As}_5\text{BiS}_{23}$  (Fig. 5).

326 According to Figure 5, the microprobe analysis of marcobaldiite agrees with a mixture of  
327 geocronite and (Sb,As)-rich kirkiite. According to its crystal structure, the kirkiite-type component  
328 is enriched in Sb relatively to As.

329 The description of marcobaldiite, characterized by a significant Bi content, similar to that  
330 reported for Bi-rich jordanite from Kirki, poses the question about the role of this element in the  
331 stabilization of the  $N = 3.5$  homologue. As a matter of fact, one could note that Bi-rich jordanite and  
332 kirkiite coexist without this intermediate new homologue and could hypothesize that the three  
333 pnictogens As, Sb, and Bi are necessary for the crystallization of marcobaldiite. However, Moëlo *et al.*  
334 (1990) found Sb-rich kirkiite, showing the simultaneous presence of these three elements; also in  
335 this case, no hints about the occurrence of marcobaldiite were found. In addition, the recent finding  
336 of the As-rich analogue of marcobaldiite, arsenmarcobaldiite (Biagioni *et al.*, 2016c), substantially  
337 devoid of Bi ( $\text{Bi} \approx 0.30$  wt%), seems to discard the hypothesis that this element plays a key role in  
338 the formation of the  $N = 3.5$  homologue.

339

### 340 **5.3. Conditions of formation**

341 The geological history of the baryte + pyrite ore deposit of the Pollone mine is very complex  
342 and its origin is still debated (Carmignani *et al.*, 1976; Costagliola *et al.*, 1998). Recently, Biagioni  
343 *et al.* (2016a) provided new details for understanding the evolution of the Pollone ore deposit.

344 Indeed, the baryte + pyrite ore bodies have been involved in the Alpine tectono-metamorphic events  
345 affecting the rocks belonging to the Apuan Alps metamorphic complex, indicating a pre-Alpine  
346 origin of the mineralization. During its late stage evolution, the formation of extension vein systems  
347 favoured the local remobilization of the ore bodies, giving rise to the peculiar sulfosalt assemblages  
348 occurring at the Pollone mine.

349 The occurrence of Bi is an unusual feature in the framework of the mineralogy of sulfosalts  
350 from Apuan Alps, since up to now very few Bi sulfosalts have been identified from the  
351 hydrothermal veins (*e.g.*, Orlandi *et al.*, 2010); at the Pollone mine, small amounts of Bi have been  
352 reported in sterrite (up to 0.26 wt% - Moëlo *et al.*, 2011) and jordanite/geocronite (up to 0.47 wt%  
353 - Biagioni *et al.*, 2016a). According to Moëlo *et al.* (1985), the elemental association of Pb, Bi, and  
354 As is typical of thermo-chemical conditions such as high  $T$  and weak  $f(S_2)$  favouring the  
355 incorporation of As as an anion in the crystallizing sulfides (*e.g.*, As-bearing pyrite or arsenopyrite).  
356 On the contrary, a high  $f(S_2)$  could allow the sulfidation of As and its occurrence in sulfosalts; such  
357 a high  $f(S_2)$  values could be achieved through the interaction between the hydrothermal solution and  
358 a pre-existing sulfide ore deposit. At the Pollone mine, the late recrystallization stage of the baryte  
359 + pyrite ore could have locally mobilized As under high  $f(S_2)$  conditions, favouring its sulfidation to  
360  $As^{3+}$  (Biagioni *et al.*, 2016a), and thus promoting the crystallization of complex Sb-As-(Bi) sulfosalt  
361 species. Since it is likely that the stabilization of the  $N = 3.5$  homologue marcobaldiite is not related  
362 to the occurrence of Bi, its crystallization could be related to small local changes in thermo-  
363 chemical conditions as well as Pb/(Sb,As,Bi) ratio, sufficient to induce the formation of distinct  
364 sulfosalts.

365 However, the question of the stabilization of marcobaldiite remains open, as this phase has  
366 not been observed in experimental studies nor in association with jordanite and kirkiite at Aghios  
367 Philippos, Kirki, Greece. Whereas kirkiite and jordanite have been synthesized (*e.g.*, Walia &  
368 Chang, 1973), no hints of the  $N = 3.5$  homologue were found in experimental studies. However, it  
369 should be noted that some old chemical analyses of jordanite homologues fit better with the  
370 composition  $Pb_{12}(Sb/As)_6S_{21}$  than with that of the  $N = 4$  homologues. As an example, Fisher (1940)  
371 reported that the old formula of jordanite was given  $Pb_4As_2S_7$ , corresponding to one third of the  
372 ideal  $Pb_{12}As_6S_{21}$  formula of a  $N = 3.5$  homologue. Likely, such discrepancies were related to  
373 inaccuracies in chemical analyses; the same composition reported for phase A of Walia & Change  
374 (1973) can be recalculated, on the basis of 6 (As+Bi) *apfu*, as  $Pb_{11.57}(As_{4.5-3.9}Bi_{1.5-2.1})S_{20.57}$ , closer to  
375  $Pb_{12}(As,Bi)_6S_{21}$  than  $Pb_{10}(As,Bi)_6S_{19}$ . In this case, the X-ray powder diffraction pattern of phase A  
376 seems to agree with that of kirkiite and not with that of marcobaldiite, even if the diffraction  
377 patterns of the jordanite homologues are very similar.

378 Owing to such limitations in old chemical analyses and the similarity in the optical  
379 properties as well as in the X-ray powder diffraction patterns with other jordanite homologues, it is  
380 likely that the presence of marcobaldiite in sulfosalt assemblages could have been overlooked.  
381 Nevertheless, at Kirki, Bi-rich jordanite appears directly in epitactic overgrowth on kirkiite, without  
382 any intermediate phase (Moëlo *et al.*, 1985). The best way to detect it is to perform single-crystal X-  
383 ray diffraction studies and systematic and accurate electron-microprobe analyses.

384

## 385 **6. Conclusion**

386 The description of marcobaldiite represents a new case of homology in the sulfosalt realm  
387 and increases the crystal-chemical complexity of the jordanite homologous series. Makovicky *et al.*  
388 (2006) predicted the possible existence of  $N = 1$ ,  $N = 2$ , and  $N = 5$  homologues within the jordanite  
389 series. Even if they have not been found yet, the discovery of the  $N = 3.5$  homologue allows us to  
390 hypothesize the existence of other kinds of combination of the  $N = 3$  and  $N = 4$  octahedral layers,  
391 similarly to what happens in the sartorite homologous series (*e.g.*, Moëlo *et al.*, 2008).

392 This finding is a further confirmation of the great mineralogical variability of the sulfosalt  
393 assemblages from the hydrothermal veins of the Apuan Alps metamorphic complex. The factors  
394 controlling the sulfosalt crystallization are not only related to the occurrence of minor components  
395 (*e.g.*, Ag, Cu, Hg, Tl), filling specific atom positions, and peculiar  $f(\text{O}_2)$  and  $f(\text{S}_2)$  conditions,  
396 promoting the crystallization of oxysulfosalts or persulfosalts; indeed, it seems likely that very  
397 subtle variations in the Pb/(Sb,As,Bi) atomic ratios in the crystallizing medium can allow the  
398 formation of distinct and original mineral species.

399

400 **Acknowledgments:** On occasion of his 80<sup>th</sup> birthday, we want to express our gratitude to Stefano  
401 Merlino, for his seminal works on mineral crystal-chemistry and modularity. This research received  
402 support by MIUR through the SIR 2014 project “THALMIGEN – Thallium: Mineralogy,  
403 Geochemistry, and Environmental Hazards”, granted to CB. The University Centrum for Applied  
404 Geosciences (UCAG) is thanked for access to the E.F. Stumpfl electron microprobe laboratory.

405

## 406 **References**

407 Baldi, M. (1982): La miniera del Pollone a Valdicastello. *Riv. Mineral. Ital.*, **6**, 46-58.  
408 Biagioni, C., Orlandi, P., Moëlo, Y., Bindi, L. (2014): Lead-antimony sulfosalts from Tuscany  
409 (Italy). XVI. Carducciite,  $(\text{AgSb})\text{Pb}_6(\text{As,Sb})_8\text{S}_{20}$ , a new Sb-rich derivative of rathite from the  
410 Pollone mine, Valdicastello Carducci: occurrence and crystal structure. *Mineral. Mag.*, **78**,  
411 1775-1793.



- 412 Biagioni, C., Dini, A., Orlandi, P., Moëlo, Y., Pasero, M., Zaccarini, F. (2016a): Lead-antimony  
413 sulfosalts from Tuscany (Italy). XX. Members of the jordanite-geocronite series from the  
414 Pollone mine, Valdicastello Carducci: occurrence and crystal structures. *Minerals*, **6**, 15.
- 415 Biagioni, C., Orlandi, P., Moëlo, Y., Stanley, C.J. (2016b): Lead-antimony sulfosalts from Tuscany  
416 (Italy). XVII. Meerschautite,  $(\text{Ag,Cu})_{5.5}\text{Pb}_{42.4}(\text{Sb,As})_{45.1}\text{S}_{112}\text{O}_{0.8}$ , a new expanded derivative of  
417 owyheeite from the Pollone mine, Valdicastello Carducci: occurrence and crystal structure.  
418 *Mineral. Mag.*, **80**, 675-690.
- 419 Biagioni, C., Merlino, S., Moëlo, Y., Pasero, M., Paar, W.H., Vezzoni, S., Zaccarini, F. (2016c):  
420 Arsenmarcobaldiite, IMA 2016-045. CNMNC Newsletter No. 33, October 2016, page 1138.  
421 *Mineral. Mag.*, **80**, 1135-1144.
- 422 Borodaev, Y.S., Garavelli, A., Kuzmina, O.V., Mozgova, N.N., Organova, N.I., Trubkin, N.V.,  
423 Vurro, F. (1998): Rare sulfosalts from Vulcano, Aeolian Islands, Italy. I. Se-bearing kirkiite,  
424  $\text{Pb}_{10}(\text{Bi,As})_6(\text{S,Se})_{19}$ . *Can. Mineral.*, **36**, 1105-1114.
- 425 Brese, N.E., O'Keeffe, M. (1991): Bond-valence parameters for solids. *Acta Crystallogr.*, **B47**,  
426 192–197.
- 427 Bryzgalov, I.A., Krivitskaya, N.N., Spiridonov, E.M. (2011): First find of the minerals of the  
428 jordanite-geocronite-schulzite series in one deposit (Darasun, Eastern Transbaikalia). *Doklady*  
429 *Earth Sci.*, **438**, 815-818.
- 430 Bruker, AXS Inc. (2004): APEX 2. Bruker Advanced X-ray Solutions, Madison, Wisconsin, USA.
- 431 Carmignani, L., Kligfield, R. (1990): Crustal extension in the northern Apennines: the transition  
432 from compression to extension in the Alpi Apuane core complex. *Tectonics*, **9**, 1275-1303.
- 433 Carmignani, L., Dessau, G., Duchi, G. (1976): Una mineralizzazione sin-tettonica: il giacimento di  
434 Valdicastello (Alpi Apuane). Rapporti fra tettonica e minerogenesi in Toscana. *Boll. Soc.*  
435 *Geol. Ital.*, **24**, 725-758.
- 436 Costagliola, P., Benvenuti, M., Lattanzi, P., Tanelli, G. (1998): Metamorphogenic barite-pyrite-(Pb-  
437 Zn-Ag) veins at Pollone, Apuan Alps, Tuscan: vein geometry, geothermobarometry, fluid  
438 inclusions and geochemistry. *Mineral. Petrol.*, **62**, 29-60.
- 439 Fisher, D.J. (1940): Discussion of “the formula of jordanite”. *Am. Mineral.*, **25**, 297-298.
- 440 Frizzo, P., Simone, S. (1995): Diaphorite in the Pollone ore deposit (Apuan Alps, Tuscany, Italy).  
441 *Eur. J. Mineral.*, **7**, 705-708.
- 442 Jambor, J.L. (1969): New lead sulfantimonides from Madoc, Ontario – Part 3 – Syntheses,  
443 paragenesis, origin. *Can. Mineral.*, **9**, 505-527.
- 444 Kerndt, T. (1845): Über die Krystallform und die chemische Zusammensetzung des Geo-Kronits  
445 von Val di Castello. *Ann. Phys.*, **141**, 302-307.

- 446 Kraus, W., Nolze, G. (1996): PowderCell – a program for the representation and manipulation of  
447 crystal structures and calculation of the resulting X-ray powder patterns. *J. Appl. Crystallogr.*,  
448 **29**, 301-303.
- 449 Makovicky, E. (1989): Modular classification of sulphosalts – current status. Definition and  
450 application of homologous series. *N. Jahrb. Miner. Abh.*, **160**, 269-297.
- 451 Makovicky, E., Balić-Žunić, T., Karanović, L., Poleti, D. (2006): The crystal structure of kirkiite,  
452  $Pb_{10}Bi_3As_3S_{19}$ . *Can. Mineral.*, **44**, 178–188.
- 453 Matsushita, Y., Momma, K., Miyawaki, R., Sato, A., Kaise, M., Kitazawa, H. (2014):  
454 Crystallographic examination of tsugaruite. IMA 2014 Abstract Volume, 331
- 455 Moëlo, Y., Oudin, E., Makovicky, E., Karup-Møller, S., Pillard, F., Bornuat, M., Evanghelou, E.  
456 (1985): La kirkiite,  $Pb_{10}Bi_3As_3S_{19}$ , une nouvelle espèce minérale homologue de la jordanite.  
457 *Bull.Minéral.*, **108**, 667–677.
- 458 Moëlo, Y., Makovicky, E., Karup- Møller, S., Cerveille, B., Maurel, C. (1990): La lévyclaude,  
459  $Pb_8Sn_7Cu_3(Bi,Sb)_3S_{28}$ , une nouvelle espèce à structure incommensurable, de la série de la  
460 cylindrite. *Eur. J. Mineral.*, **2**, 711-723.
- 461 Moëlo, Y., Makovicky, E., Mozgova, N.N., Jambor, J.L., Cook, N., Pring., A., Paar, W.H., Nickel,  
462 E.H., Graeser, S., Karup-Møller, S., Balić-Žunić, T., Mumme, W.G., Vurro, F., Topa, D.,  
463 Bindi, L., Bente, K., Shimizu, M. (2008): Sulfosalt systematics: a review. Report of the  
464 sulfosalt sub-committee of the IMA Commission on Ore Mineralogy. *Eur. J. Mineral.*, **20**, 7–  
465 46.
- 466 Moëlo, Y., Orlandi, P., Guillot-Deudon, C., Biagioni, C., Paar, W., Evain, M. (2011): Lead-  
467 antimony sulfosalts from Tuscany (Italy). XI. The new mineral species parasterryite,  
468  $Ag_4Pb_{20}(Sb_{14.5}As_{9.5})_{\Sigma 24}S_{58}$ , and associated sterryite,  $Cu(Ag,Cu)_3Pb_{19}(Sb,As)_{22}(As-As)S_{56}$ ,  
469 from the Pollone mine, Tuscany, Italy. *Can. Mineral.*, **49**, 623-638.
- 470 Orlandi, P., Moëlo, Y., Biagioni, C. (2010): Lead-antimony sulfosalts from Tuscany (Italy). X.  
471 Dadsonite from the Buca della Vena mine and Bi-rich izoklakeite from the Seravezza marble  
472 quarries. *Per. Mineral.*, **79**, 113-121.
- 473 Pinto, D., Balić-Žunić, T., Garavelli, A., Garbarino, C., Makovicky, E., Vurro, F. (2006): First  
474 occurrence of close-to-ideal kirkiite at Vulcano (Aeolian Islands, Italy): chemical data and  
475 single-crystal X-ray study. *Eur. J. Mineral.*, **18**, 393-401.
- 476 Sheldrick, G.M. (2008): A short history of SHELX. *Acta Crystallogr.*, **A64**, 112-122.
- 477 Sheldrick, G.M. (2015): Crystal structure refinement with SHELXL. *Acta Crystallogr.*, **C71**, 3-8.

- 478 Shimizu, M., Miyawaki, R., Kato, A., Matsubara, F., Matsuyama, F., Kiyota, K. (1998):  
479 Tsugaruite,  $Pb_4As_2S_7$ , a new mineral species from the Yunosawa mine, Aomori Prefecture,  
480 Japan. *Mineral. Mag.*, **62**, 793-799.
- 481 Topa, D., Keutsch, F.N., Makovicky, E., Kolitsch, U., Paar, W. (2017): Polloneite, a new complex  
482 Pb(-Ag)-As-Sb sulfosalt from the Pollone mine, Apuan Alps, Tuscany, Italy. *Mineral. Mag.*,  
483 in press.
- 484 Walia, D.S., Chang, L.L.Y. (1973): Investigations in the systems  $PbS-Sb_2S_3-As_2S_3$  and  $PbS-Bi_2S_3-$   
485  $As_2S_3$ . *Can. Mineral.*, **12**, 113-119.
- 486 Wilson, A.J.C., Ed. (1992): *International Tables for X-ray Crystallography*, Volume C:  
487 Mathematical, physical and chemical tables. Kluwer Academic, Dordrecht, NL.  
488

489 **Table captions**

490 **Table 1** – Sulfosalts identified in the Pollone ore deposit. In bold, minerals having their type  
491 locality at the Pollone mine.

492 **Table 2** – Reflectance data (%) for marcobaldiite in air.

493 **Table 3** – Electron microprobe analysis of marcobaldiite: chemical composition as wt% (10 spot  
494 analyses) and number of atoms per formula unit (apfu) on the basis of  $\Sigma Me = 18$  apfu.

495 **Table 4** – X-ray powder diffraction data for marcobaldiite. Intensities and  $d_{hkl}$  were calculated using  
496 the software *PowderCell 2.3* (Kraus and Nolze, 1996) on the basis of the structural model given in  
497 Table 5. The six strongest reflections are given in bold. Only reflections with  $I_{calc} \geq 5$  were  
498 reported, if not observed. Observed intensities were visually estimated (vs = very strong; s = strong;  
499 ms = medium-strong; m = medium; mw = medium-weak; w = weak; vw = very weak).

500 **Table 5** – Crystal data and summary of parameters describing data collection and refinement for  
501 marcobaldiite.

502 **Table 6** – Atomic coordinates, site occupancy factor (s.o.f.), and equivalent isotropic displacement  
503 parameters ( $\text{\AA}^2$ ) for marcobaldiite.

504 **Table 7** – Coordination number (C.N.), mean bond distance  $\langle Me-S \rangle$  ( $\text{\AA}$ ), and bond-valence sums  
505 (BVS – in valence unit, *v.u.*) for cation sites in marcobaldiite.

506 **Table 8** – Bond valence sums (BVS – in valence unit, *v.u.*) for S atoms in marcobaldiite.

507 **Table 9** – Comparison between site labels and site occupancy factors (s.o.f.) in marcobaldiite,  
508 kirkiite, and jordanite/geocronite isotypes.

509

510 **Figure captions**

511 **Figure 1** – Reflected light microscopy image of marcobaldiite, showing polysynthetic twinning.  
512 Holotype material, Natural History Museum of Pisa University, catalogue number # 19709.

513 **Figure 2** – Projection along *c* of the crystal structure of marcobaldiite.

514 **Figure 3** – Modular organization of the crystal structure of marcobaldiite. Alternating oblique  $N = 3$   
515 and  $N = 4$  layers are separated by single slabs TP of trigonal prismatic Pb and split As17a/As17b.  
516 The three shortest (Sb,As)–S and (Pb,Sb)–S bonds have been enhanced. Shaded ellipses: lone-  
517 electron-pair micelles of trivalent Sb and As.

518 **Figure 4** – Comparison between  $N = 3$  and  $N = 4$  octahedral layers of marcobaldiite with those  
519 occurring in kirkiite (a) and jordanite/geocronite (b).

520 **Figure 5** – Projection in the As-Sb-Bi sub-system of various compositions within the jordanite  
521 homologous series. Homologues: N = 3, pink squares (kirkiite); N = 4, yellow triangles (jordanite  
522 and geocronite); N = 3.5, blue lozenges (marcobaldiite and arsenmarcobaldiite). EPMA:  
523 microprobe analysis; STR: crystal structure, with L3: composition of the kirkiite sub-part (= L3  
524 layer + intermediate slab), and L4: composition of the geocronite sub-part.

525

526

527 **Table 1** – Sulfosalts identified in the Pollone ore deposit. In bold, minerals having their type  
 528 locality at the Pollone mine.

Mineral	Chemical formula	Mineral	Chemical formula
Boulangerite	Pb <sub>5</sub> Sb <sub>4</sub> S <sub>11</sub>	Owyheeite	Ag <sub>3</sub> Pb <sub>10</sub> Sb <sub>11</sub> S <sub>28</sub>
Bournonite	CuPbSbS <sub>3</sub>	<b>Parasterryite</b>	Ag <sub>4</sub> Pb <sub>20</sub> (Sb,As) <sub>24</sub> S <sub>58</sub>
<b>Carducciite</b>	(AgSb)Pb <sub>6</sub> (As,Sb) <sub>8</sub> S <sub>20</sub>	<b>Polloneite</b>	AgPb <sub>46</sub> As <sub>26</sub> Sb <sub>23</sub> S <sub>120</sub>
Chovanite	Pb <sub>28</sub> (Sb,As) <sub>30</sub> S <sub>72</sub> O	Proustite	Ag <sub>3</sub> AsS <sub>3</sub>
Diaphorite	Ag <sub>3</sub> Pb <sub>2</sub> Sb <sub>3</sub> S <sub>8</sub>	Pyrargyrite	Ag <sub>3</sub> SbS <sub>3</sub>
Ferdowsiite	Ag <sub>8</sub> Sb <sub>5</sub> As <sub>3</sub> S <sub>16</sub>	Seligmannite	CuPbAsS <sub>3</sub>
Fettelite	[Ag <sub>6</sub> As <sub>2</sub> S <sub>7</sub> ][Ag <sub>10</sub> HgAs <sub>2</sub> S <sub>8</sub> ]	Sterryite	Cu(Ag,Cu) <sub>3</sub> Pb <sub>19</sub> (Sb,As) <sub>22</sub> (As–As) <sub>5</sub> S <sub>56</sub>
Geocronite	Pb <sub>14</sub> Sb <sub>6</sub> S <sub>23</sub>	Tennantite	Cu <sub>6</sub> Cu <sub>4</sub> (Fe,Zn) <sub>2</sub> As <sub>4</sub> S <sub>13</sub>
Jordanite	Pb <sub>14</sub> As <sub>6</sub> S <sub>23</sub>	Tetrahedrite	Cu <sub>6</sub> Cu <sub>4</sub> (Fe,Zn) <sub>2</sub> Sb <sub>4</sub> S <sub>13</sub>
<b>Marcobaldiite</b>	Pb <sub>12</sub> (Sb <sub>3</sub> As <sub>2</sub> Bi) <sub>Σ6</sub> S <sub>23</sub>	Twinnite	PbSbAsS <sub>4</sub>
<b>Meerschautite</b>	(Ag,Cu) <sub>5.5</sub> Pb <sub>42.4</sub> (Sb,As) <sub>45.1</sub> S <sub>112</sub> O <sub>0.8</sub>	Xanthoconite	Ag <sub>3</sub> AsS <sub>3</sub>
Meneghinite	CuPb <sub>13</sub> Sb <sub>7</sub> S <sub>24</sub>	Zinkenite	Pb <sub>9</sub> Sb <sub>22</sub> S <sub>42</sub>

529

530 **Table 2** – Reflectance data (%) for marcobaldiite in air.

λ/nm	R <sub>min</sub>	R <sub>max</sub>	λ/nm	R <sub>min</sub>	R <sub>max</sub>
400	31.2	35.2	560	30.6	39.0
420	32.3	39.7	580	30.4	38.5
440	32.7	41.7	<b>589</b>	<b>30.4</b>	<b>38.5</b>
460	31.8	40.2	600	30.1	38.4
<b>470</b>	<b>31.6</b>	<b>40.1</b>	620	30.1	38.1
480	31.8	40.1	640	30.2	38.0
500	31.4	39.9	<b>650</b>	<b>30.0</b>	<b>37.6</b>
520	31.1	39.5	660	29.9	37.6
540	31.0	39.5	680	29.6	36.9
<b>546</b>	<b>30.9</b>	<b>39.6</b>	700	29.1	36.4

531

532

533 **Table 3** – Electron microprobe analysis of marcobaldiite: chemical composition as wt% (10 spot  
 534 analyses) and number of atoms per formula unit (apfu) on the basis of  $\Sigma Me = 18$  apfu.

Element	wt%	range	e.s.d.
Pb	64.05	63.52 – 64.46	0.34
Bi	4.24	4.16 – 4.35	0.06
Sb	9.10	8.89 – 9.38	0.14
As	4.51	4.35 – 4.62	0.08
S	17.24	16.89 – 17.42	0.19
Total	99.14	98.29 – 100.02	0.53
<hr/>			
apfu ( <i>Me</i> = 18)			
Pb	11.98	11.91 – 12.06	0.04
Bi	0.79	0.77 – 0.80	0.01
Sb	2.90	2.84 – 2.96	0.03
As	2.33	2.27 – 2.40	0.03
S	20.80	20.47 – 21.11	0.20
<i>Ev</i> (%)	0.8	-0.5 – 2.6	1.1

$$Ev (\%) = [\Sigma(val+) - \Sigma(val-)] \times 100 / \Sigma(val-).$$

535

536

537 **Table 4** –X-ray powder diffraction data for marcobaldite. Intensities and  $d_{hkl}$  were calculated using  
 538 the software *PowderCell 2.3* (Kraus and Nolze, 1996) on the basis of the structural model given in  
 539 Table 5. The eight strongest reflections are given in bold. Only reflections with  $I_{calc} \geq 5$  were  
 540 reported, if not observed. Observed intensities were visually estimated (vs = very strong; s = strong;  
 541 ms = medium-strong; m = medium; mw = medium-weak; w = weak; vw = very weak).

$l_{obs}$	$d_{obs}$	$l_{calc}$	$d_{calc}$	$hkl$	$l_{obs}$	$d_{obs}$	$l_{calc}$	$d_{calc}$	$hkl$		
w	4.45	8	4.406	-2 1 1	vw	2.553	8	2.568	-1 -10 2		
w	3.835	25	3.832	2 1 0	w	2.489	5	2.496	-2 8 2		
w	3.737	6	3.756	2 -3 0	vw	2.442	3	2.434	-2 10 1		
		5	3.735	-2 -1 2	mw	2.388	2	2.391	0 8 2		
		45	3.692	2 2 0			2	2.385	-2 -10 2		
		18	3.683	-2 -2 2	vw	2.347	1	2.342	1 -9 2		
		20	3.676	0 -3 2	w	2.294	1	2.297	1 6 2		
ms	3.568	7	3.596	0 1 2	vs	2.233	5	2.241	-1 10 2		
		21	3.591	2 -4 0			48	2.240	2 -2 2		
		25	3.577	-2 -3 2			6	2.240	-2 -11 2		
		40	3.555	0 -4 2			6	2.229	2 10 0		
m	3.404	17	3.448	0 2 2	s	2.125	5	2.204	0 -12 2		
		17	3.431	-2 -4 2			46	2.203	-4 2 2		
		26	3.398	2 -5 0			7	2.118	3 7 0		
		11	3.398	0 -5 2			54	2.110	-2 0 4		
m	3.256	14	3.384	-2 3 2	vw	2.072	13	2.074	0 -13 2		
		28	3.314	2 4 0			w	2.035	3	2.028	3 8 0
		19	3.274	0 3 2			w	2.020	5	2.022	2 -13 0
		52	3.259	-2 -5 2			mw	1.980	6	1.986	-2 -13 2
ms	3.202	100	3.219	0 9 0	mw	1.950	20	1.957	-4 -7 2		
		27	3.219	0 -6 2			6	1.956	0 -14 2		
		30	3.208	-2 4 2			8	1.916	4 2 0		
m	3.075	29	3.109	2 5 0	mw	1.911	6	1.906	2 -14 0		
		9	3.088	0 4 2			20	1.895	-2 -9 4		
		30	3.075	-2 -6 2			6	1.880	0 12 2		
ms	3.016	28	3.032	0 -7 2	m	1.878	6	1.868	-4 -2 4		
		12	3.023	-2 5 2			9	1.847	-2 13 2		
ms	2.885	35	2.991	2 -7 0	s	1.848	17	1.843	2 -11 2		
		13	2.908	2 6 0			7	1.839	4 -7 0		
m	2.832	36	2.902	0 5 2	vw	1.797	16	1.835	2 7 2		
		10	2.846	0 -8 2			7	1.811	0 -7 4		
w	2.789	28	2.795	2 -8 0	vw	1.797	6	1.798	0 2 4		
vw	2.756	4	2.755	1 -5 2	s	1.775	5	1.778	0 -8 4		
mw	2.707	22	2.721	0 6 2	w	1.753	5	1.749	-2 14 2		
		5	2.720	1 2 2	w	1.716	12	1.705	-4 11 2		
vw	2.652	19	2.662	-2 7 2	w	1.661	12	1.658	-2 9 2		
w	2.606	6	2.612	2 -9 0	w	1.608	12	1.609	0 18 0		

542

543



544 **Table 5** – Crystal data and summary of parameters describing data collection and refinement for  
 545 marcobaldiite.  
 546

<b>Crystal data</b>	
Crystal size (mm <sup>3</sup> )	0.09 x 0.08 x 0.04
Cell setting, space group	Triclinic, <i>P</i> -1
<i>a</i> (Å)	8.9248(9)
<i>b</i> (Å)	29.414(3)
<i>c</i> (Å)	8.5301(8)
$\alpha$ (°)	98.336(5)
$\beta$ (°)	118.175(5)
$\gamma$ (°)	90.856(5)
<i>V</i> (Å <sup>3</sup> )	1944.1(3)
<i>Z</i>	2
<b>Data collection and refinement</b>	
Radiation, wavelength (Å)	Mo K $\alpha$ , $\lambda$ = 0.71073
Temperature (K)	293
$2\theta_{\max}$ (°)	50.29
Measured reflections	41210
Unique reflections	6790
Reflections with $F_o > 4\sigma(F_o)$	6188
$R_{\text{int}}$	0.0409
$R\sigma$	0.0269
Range of <i>h, k, l</i>	$-10 \leq h \leq 10,$ $-34 \leq k \leq 34,$ $-10 \leq l \leq 10$
$R [F_o > 4\sigma(F_o)]$	0.0668
$R$ (all data)	0.0702
$wR$ (on $F_o^2$ )	0.2228
Goof	1.093
Number of least-squares parameters	363
Maximum and minimum residual peak (e Å <sup>-3</sup> )	10.88 (at 0.97 Å from Pb5) -3.76 (at 1.05 Å from S18)

547 **Table 6** – Atomic coordinates, site occupancy factor (s.o.f.), and equivalent isotropic displacement  
 548 parameters ( $\text{\AA}^2$ ) for marcobaldiite.

Site	s.o.f.	$x/a$	$y/b$	$z/c$	$U_{eq}$
Pb1	Pb <sub>0.85</sub> Bi <sub>0.15</sub>	0.8503(1)	0.38701(4)	0.4904(2)	0.0199(3)
Pb2	Pb <sub>1.00</sub>	0.8518(1)	0.38638(4)	0.9939(2)	0.0199(3)
Pb3	Pb <sub>1.00</sub>	0.2253(1)	0.49413(4)	0.7368(2)	0.0213(3)
Sb4	Sb <sub>1.00</sub>	0.2412(2)	0.50143(6)	0.2478(2)	0.0116(4)
As5	As <sub>0.63(3)</sub> Sb <sub>0.37(3)</sub>	0.3689(3)	0.39399(8)	0.0047(3)	0.0171(8)
Pb6	Pb <sub>1.00</sub>	0.3821(2)	0.39554(4)	0.5075(2)	0.0258(3)
Pb7	Pb <sub>1.00</sub>	0.7725(1)	0.16711(4)	0.8456(1)	0.0192(3)
Pb8	Pb <sub>0.85</sub> Bi <sub>0.15</sub>	0.7695(1)	0.16641(4)	0.3381(2)	0.0194(3)
Pb9	Pb <sub>0.61(1)</sub> Sb <sub>0.39(1)</sub>	0.0830(2)	0.05688(5)	0.9425(2)	0.0230(3)
Pb10	Pb <sub>1.00</sub>	0.0780(1)	0.05992(4)	0.4471(2)	0.0195(3)
Pb11	Pb <sub>1.00</sub>	0.6128(1)	0.04819(4)	0.9512(2)	0.0201(3)
Sb12	Sb <sub>0.98(3)</sub> As <sub>0.02(3)</sub>	0.5985(2)	0.05375(6)	0.4500(2)	0.0146(6)
As13	As <sub>0.91(3)</sub> Sb <sub>0.09(3)</sub>	0.2850(3)	0.15729(9)	0.8444(4)	0.0157(9)
Pb14	Pb <sub>1.00</sub>	0.2937(2)	0.16075(4)	0.3477(2)	0.0243(3)
Pb15	Pb <sub>0.85</sub> Bi <sub>0.15</sub>	0.4812(2)	0.27712(4)	0.2586(2)	0.0238(3)
Pb16	Pb <sub>0.85</sub> Bi <sub>0.15</sub>	0.4818(2)	0.27741(4)	0.7431(2)	0.0249(3)
As17a	As <sub>0.75(1)</sub>	0.9939(4)	0.30213(11)	0.2707(4)	0.0146(7)
As17b	As <sub>0.25(1)</sub>	0.9756(12)	0.2494(3)	0.2340(14)	0.0146(7)
Pb18	Pb <sub>1.00</sub>	0.0467(2)	0.27511(4)	0.7796(2)	0.0347(4)
S1	S <sub>1.00</sub>	0.6054(8)	0.3514(2)	0.0996(8)	0.0161(12)
S2	S <sub>1.00</sub>	0.6316(8)	0.3389(2)	0.6100(8)	0.0162(12)
S3	S <sub>1.00</sub>	0.0088(8)	0.4443(2)	0.3618(8)	0.0175(13)
S4	S <sub>1.00</sub>	0.9991(8)	0.4492(2)	0.8435(8)	0.0150(12)
S5	S <sub>1.00</sub>	0.6084(8)	0.4537(2)	0.4324(8)	0.0159(12)
S6	S <sub>1.00</sub>	0.6113(8)	0.4537(2)	0.8754(8)	0.0145(12)
S7	S <sub>1.00</sub>	0.2267(8)	0.3527(2)	0.1134(9)	0.0216(13)
S8	S <sub>1.00</sub>	0.2236(9)	0.3538(2)	0.7092(9)	0.0227(14)
S9	S <sub>1.00</sub>	0.5456(8)	0.1986(2)	0.9932(8)	0.0150(12)
S10	S <sub>1.00</sub>	0.5942(8)	0.2136(2)	0.5278(8)	0.0166(12)
S11	S <sub>1.00</sub>	0.8941(9)	0.1089(2)	0.1302(9)	0.0189(13)
S12	S <sub>1.00</sub>	0.8730(8)	0.1013(2)	0.6092(8)	0.0148(12)
S13	S <sub>1.00</sub>	0.1968(8)	0.0032(2)	0.2106(9)	0.0169(12)
S14	S <sub>1.00</sub>	0.1985(8)	0.0050(2)	0.7444(8)	0.0167(12)
S15	S <sub>1.00</sub>	0.4821(8)	0.0967(2)	0.6306(8)	0.0153(12)
S16	S <sub>1.00</sub>	0.4785(8)	0.0960(2)	0.1916(8)	0.0159(12)
S17	S <sub>1.00</sub>	0.1671(9)	0.1958(2)	0.6078(9)	0.0236(14)
S18	S <sub>1.00</sub>	0.1711(8)	0.1962(2)	0.0017(9)	0.0205(13)
S19	S <sub>1.00</sub>	0.8506(8)	0.2722(2)	0.3915(9)	0.0222(14)
S20	S <sub>1.00</sub>	0.8518(8)	0.2734(2)	0.9742(9)	0.0196(13)
S21a	S <sub>0.75(1)</sub>	0.2244(10)	0.2630(3)	0.3651(10)	0.0111(15)
S21b	S <sub>0.25(1)</sub>	0.233(3)	0.2882(10)	0.381(3)	0.0111(15)

549

550 **Table 7** – Coordination number (C.N.), mean bond distance  $\langle Me-S \rangle$  (Å), and bond-valence sums  
 551 (BVS – in valence unit,  $v.u.$ ) for cation sites in marcobaldiite.

Site	s.o.f.	C.N.	$\langle Me-S \rangle$	BVS	Site	s.o.f.	C.N.	$\langle Me-S \rangle$	BVS
Pb1	Pb <sub>0.85</sub> Bi <sub>0.15</sub>	VII	3.031	2.10	Pb10	Pb <sub>1.00</sub>	VI	2.996	1.95
Pb2	Pb <sub>1.00</sub>	VII	3.050	1.95	Pb11	Pb <sub>1.00</sub>	VI	3.016	1.95
Pb3	Pb <sub>1.00</sub>	VI	3.012	1.99	Sb12	Sb <sub>0.98</sub> As <sub>0.02</sub>	III+III	2.462	3.14
Sb4	Sb <sub>1.00</sub>	III+III*	2.504**	2.94	As13	As <sub>0.91</sub> Sb <sub>0.09</sub>	III	2.262	3.11
As5	As <sub>0.63</sub> Sb <sub>0.37</sub>	III	2.325	3.15	Pb14	Pb <sub>1.00</sub>	VII	3.046***	2.02
Pb6	Pb <sub>1.00</sub>	VII	3.055***	1.97	Pb15	Pb <sub>0.85</sub> Bi <sub>0.15</sub>	VIII	3.073	2.10
Pb7	Pb <sub>1.00</sub>	VII	3.024	2.00	Pb16	Pb <sub>0.85</sub> Bi <sub>0.15</sub>	VIII	3.075	2.10
Pb8	Pb <sub>0.85</sub> Bi <sub>0.15</sub>	VII	3.013	2.08	As17a	As <sub>0.75</sub>	III	2.233	3.22
Pb9	Pb <sub>0.61</sub> Sb <sub>0.39</sub>	VI	2.922	2.35	As17b	As <sub>0.25</sub>	III	2.191	3.52
Pb10	Pb <sub>1.00</sub>	VI	2.996	1.95	Pb18	Pb <sub>1.00</sub>	VI	3.023	1.75

\* 3 short and 3 longer bonds. \*\* Mean of the 3 short bonds. \*\*\* Calculated assuming the full occupancy of S21b and S21a for Pb6 and Pb14, respectively

552

553 **Table 8** – Bond valence sums (BVS – in valence unit,  $v.u.$ ) for S atoms in marcobaldiite.

Site	BVS	Site	BVS
S1	2.06	S12	2.09
S2	2.06	S13	1.93
S3	2.02	S14	2.01
S4	2.03	S15	1.97
S5	1.91	S16	1.92
S6	1.95	S17	1.88
S7	1.96	S18	1.95
S8	1.89	S19	2.21
S9	1.96	S20	2.13
S10	1.98	S21a	2.11
S11	2.00	S21b	2.08

554

555

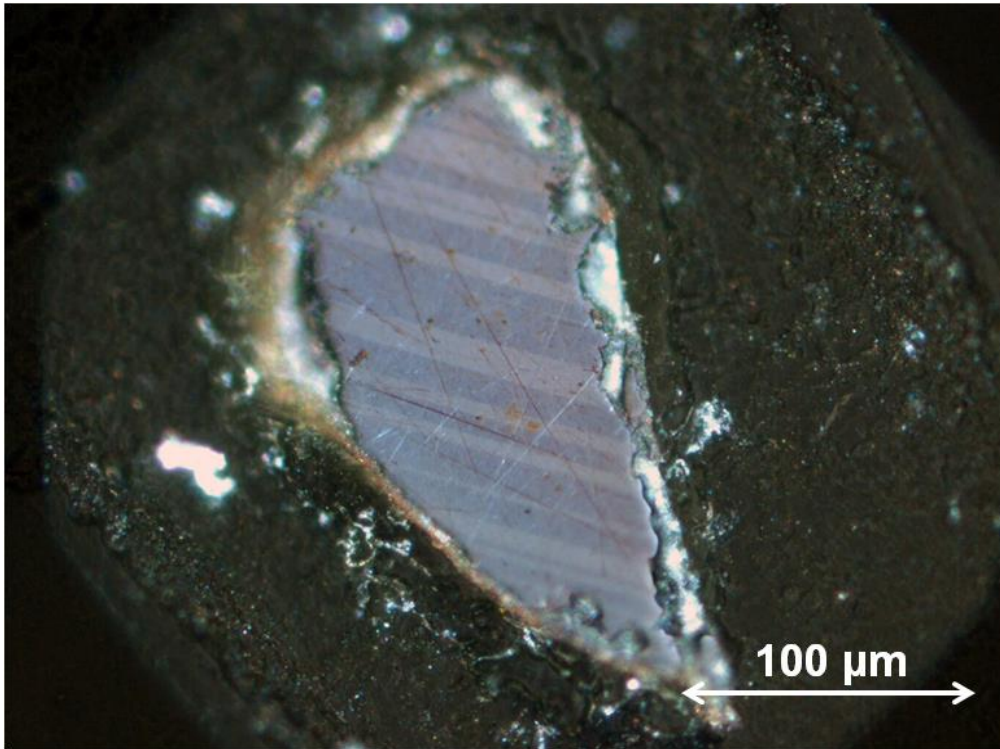
556

557 **Table 9** – Comparison between site labels and site occupancy factors (s.o.f.) in marcobaldiite,  
 558 kirkiite, and jordanite/geocronite isotypes.

Marcobaldiite		Kirkiite		Jordanite/geocronite	
Site	s.o.f.	Site	s.o.f.	Site	s.o.f.
Pb1	Pb <sub>0.85</sub> Bi <sub>0.15</sub>	Pb4	Pb <sub>0.75</sub> Bi <sub>0.25</sub>		
Pb2	Pb <sub>1.00</sub>	Pb3	Pb <sub>1.00</sub>		
Pb3	Pb <sub>1.00</sub>	Pb1	Pb <sub>1.00</sub>		
Sb4	Sb <sub>1.00</sub>	Bi1/As1	Bi <sub>0.58</sub> /As <sub>0.42</sub>		
As5	As <sub>0.63</sub> Sb <sub>0.37</sub>	As2	As <sub>1.00</sub>		
Pb6	Pb <sub>1.00</sub>	Pb2	Pb <sub>1.00</sub>		
Pb7	Pb <sub>1.00</sub>			Pb7	Pb <sub>1.00</sub>
Pb8	Pb <sub>0.85</sub> Bi <sub>0.15</sub>			Pb8	Pb <sub>1.00</sub>
Pb9	Pb <sub>0.61</sub> Sb <sub>0.39</sub>			Pb2/Sb2	Pb <sub>0.50</sub> /Sb <sub>0.50</sub>
Pb10	Pb <sub>1.00</sub>			Pb1	Pb <sub>1.00</sub>
Pb11	Pb <sub>1.00</sub>			Pb3	Pb <sub>1.00</sub>
Sb12	Sb <sub>0.98</sub> As <sub>0.02</sub>			Sb4	Sb <sub>0.61-0.98</sub> As <sub>0.39-0.02</sub>
As13	As <sub>0.91</sub> Sb <sub>0.09</sub>			As6	As <sub>1.00-0.75</sub> Sb <sub>0.00-0.25</sub>
Pb14	Pb <sub>1.00</sub>			Pb5	Pb <sub>1.00</sub>
Pb15	Pb <sub>0.85</sub> Bi <sub>0.15</sub>	Pb7	Pb <sub>1.00</sub>	Pb9	Pb <sub>1.00</sub>
Pb16	Pb <sub>0.85</sub> Bi <sub>0.15</sub>	Pb6	Pb <sub>0.5</sub> Bi <sub>0.5</sub>	Pb10	Pb <sub>1.00</sub>
As17	As <sub>1.00</sub>	As3	As <sub>1.00</sub>	As11	As <sub>1.00</sub>
Pb18	Pb <sub>1.00</sub>	Pb5	Pb <sub>1.00</sub>	Pb12	Pb <sub>1.00</sub>

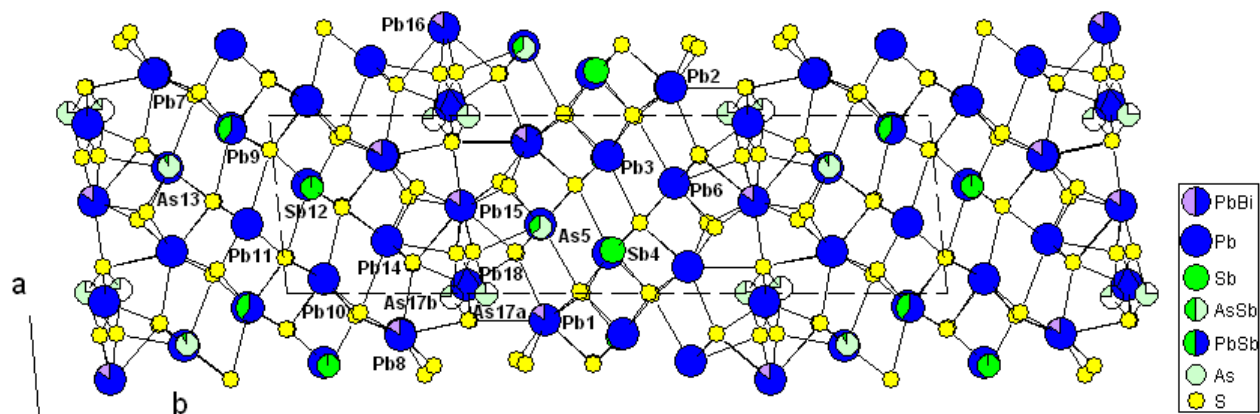
559 Note: s.o.f. for kirkiite and jordanite/geocronite after Makovicky *et al.* (2006) and Biagioni *et al.* (2016a),  
 560 respectively.

561 **Figure 1** – Reflected light microscopy image of marcobaldiite, showing polysynthetic twinning.  
562 Holotype material, Natural History Museum of Pisa University, catalogue number # 19709.



563  
564

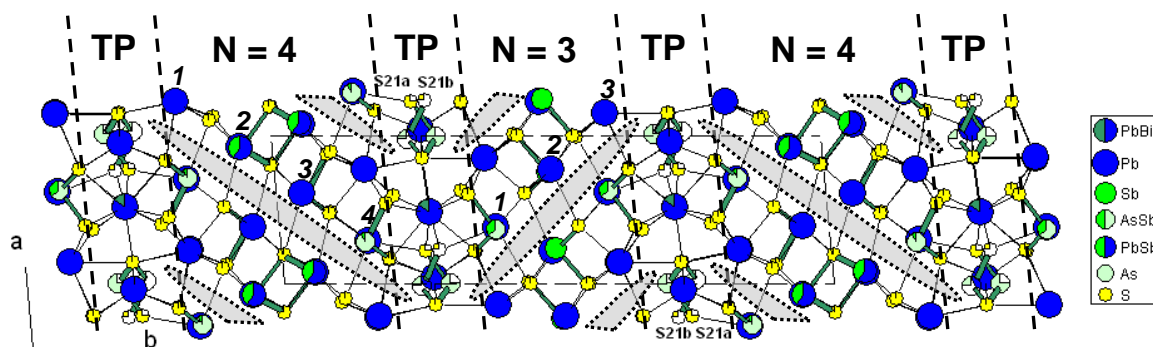
565 **Figure 2** – Projection along *c* of the crystal structure of marcobaldiite.



566

567

568 **Figure 3** – Modular organization of the crystal structure of marcobaldiite. Alternating oblique  $N = 3$   
 569 and  $N = 4$  layers are separated by single slabs TP of trigonal prismatic Pb and split As17a/As17b.  
 570 The three shortest (Sb,As)–S and (Pb,Sb)–S bonds have been enhanced. Shaded ellipses: lone-  
 571 electron-pair micelles of trivalent Sb and As.

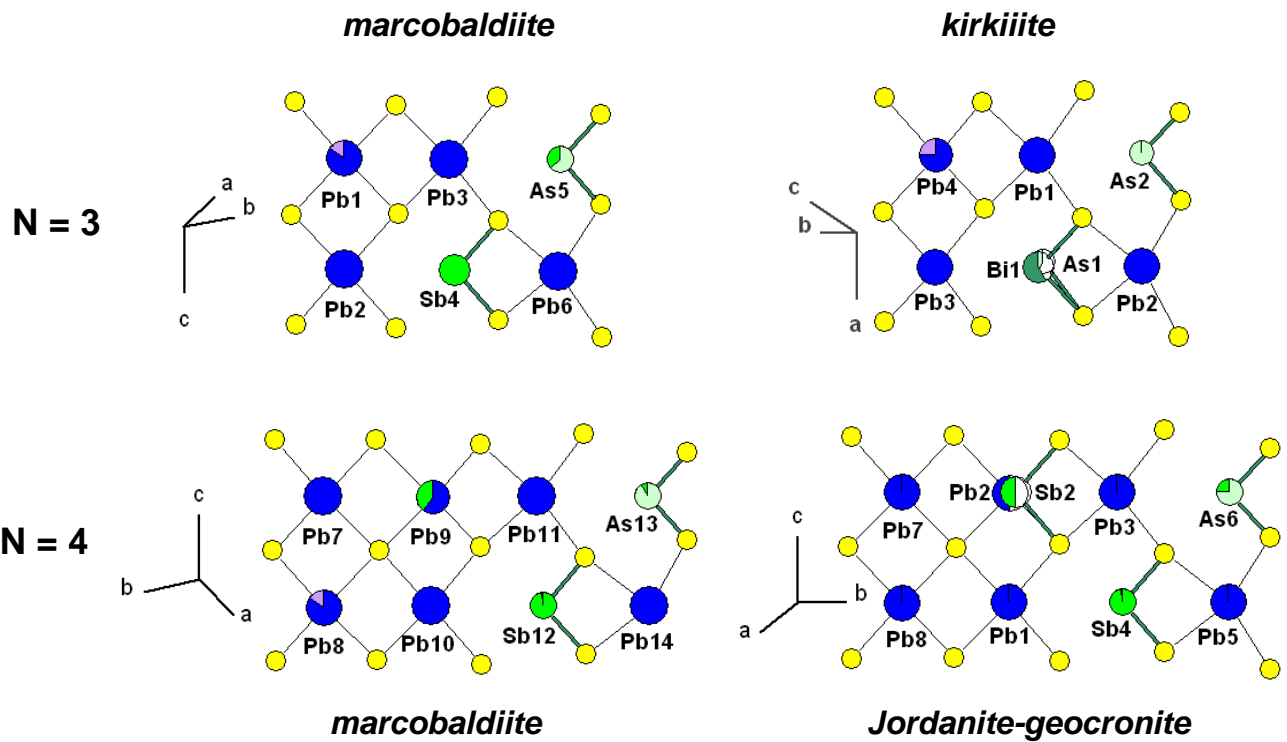


572

573

574

575 **Figure 4** – Comparison between  $N = 3$  and  $N = 4$  octahedral layers of marcobaldiite with those  
 576 occurring in kirkiite (top) and jordanite/geocronite (bottom).



577

578



579 **Figure 5** – Projection in the As-Sb-Bi sub-system of various compositions within the jordanite  
 580 homologous series. Homologues: N = 3, pink squares (kirkiite); N = 4, yellow triangles (jordanite  
 581 and geocronite); N = 3.5, blue lozenges (marcobaldiite and arsenmarcobaldiite). EPMA:  
 582 microprobe analysis; STR: crystal structure, with L3: composition of the kirkiite sub-part (= L3  
 583 layer + intermediate slab), and L4: composition of the geocronite sub-part.

